

## DIRECT CONSTRAINTS ON THE DARK MATTER SELF-INTERACTION CROSS-SECTION FROM THE MERGING CLUSTER 1E 0657-56

M. MARKEVITCH<sup>1</sup>, A. H. GONZALEZ<sup>2</sup>, D. CLOWE<sup>3</sup>, A. VIKHLININ<sup>1,4</sup>, L. DAVID<sup>1</sup>, W. FORMAN<sup>1</sup>, C. JONES<sup>1</sup>, S. MURRAY<sup>1</sup>,  
W. TUCKER<sup>1,5</sup>*Submitted to ApJ*

## ABSTRACT

We compare new maps of the hot gas, dark matter, and galaxies for 1E 0657-56, a cluster with a rare, high-velocity merger occurring nearly in the plane of the sky. The X-ray observations reveal a bullet-like gas subcluster just exiting the collision site. A prominent bow shock gives an estimate of the subcluster velocity, 4500 km s<sup>-1</sup>. The optical image shows that the gas lags behind the subcluster galaxies. The weak-lensing mass map reveals a dark matter clump lying ahead of the collisional gas bullet, but coincident with the effectively collisionless galaxies. From these observations, one can directly estimate the cross-section of the dark matter self-interaction. That the dark matter is not fluid-like can be seen directly from the maps; more quantitative limits can be derived from four simple independent arguments. The most sensitive constraint,  $\sigma/m < 1 \text{ cm}^2 \text{ g}^{-1}$ , comes from the consistency of the subcluster mass-to-light ratio with the main cluster (and universal) value, which rules out a large mass loss due to dark matter particle collisions. This limit excludes most of the 0.5–5 cm<sup>2</sup> g<sup>-1</sup> interval proposed to explain the flat mass profiles in galaxies. Our result is only an order-of-magnitude estimate which involves a number of conservative simplifying assumptions; stronger constraints may be derived using hydrodynamic simulations of this cluster.

*Subject headings:* dark matter — galaxies: clusters: individual (1E0657-56) — galaxies: formation — large scale structure of universe

## 1. INTRODUCTION

1E 0657-56, one of the hottest and most luminous clusters known, was discovered by Tucker et al. (1995). It was first observed by *Chandra* in October 2000 for 24 ks. That observation revealed a bullet-like, relatively cool subcluster just exiting the core of the main cluster, with a prominent bow shock (Markevitch et al. 2002, hereafter M02). A comparison of the X-ray and optical images revealed a galaxy subcluster just ahead of the gas “bullet”, which led M02 to suggest that this unique system could be used to determine whether dark matter is collisional or collisionless, if only one could map the mass distribution in the subcluster. Apart from the obvious basic interest for the still unknown nature of dark matter, the possibility of it having a nonzero self-interaction cross-section has far-reaching astrophysical implications (Spergel & Steinhardt 2000; for a more detailed discussion see §3.1 below).

Just such a map of the dark matter distribution in 1E 0657-56 has been obtained by Clowe et al. (in prep., hereafter C03) from weak lensing data. It reveals a dark matter clump coincident with the centroid of the galaxies (Fig. 1a). In addition, *Chandra* re-observed 1E 0657-56 for 70 ks in July 2002, from which a more accurate estimate of the shock Mach number was derived using the gas density jump at the shock,  $M = 3.2_{-0.6}^{+0.8}$  (all uncertainties 68%), which corresponds to a shock (and bullet subcluster) velocity of  $v_s = 4500_{-800}^{+1100}$  km s<sup>-1</sup> (Markevitch et al., in prep., hereafter M03). The new X-ray data also clarified the geometry of the merger. The X-

ray image (Fig. 1b), the gas temperature map (M03) and its comparison with the radio halo map (Liang et al. 2000), all suggest that the subcluster has passed very close to the center of the main cluster, at least in projection. The radial and sky plane components of the present subcluster velocity (Barrena et al. 2002 and M02, respectively), as well as the sharpness of the shock front, indicate that the subcluster is currently moving very nearly in the plane of the sky. Moreover, a cooler North-South bar in the X-ray image between the two dark matter subclusters appears to be a pancake-like remnant of the subcluster’s outer atmosphere seen edge-on (M03), suggesting that the subcluster has indeed passed through the core in three dimensions.

In this paper, we combine these new data to constrain the self-interaction cross-section of dark matter particles. We use  $\Omega_0 = 0.3$ ,  $\Omega_\Lambda = 0.7$ ,  $H_0 = 70 \text{ km s}^{-1} \text{ Mpc}^{-1}$ , for which  $1'' = 4.42 \text{ kpc}$  at the cluster redshift  $z = 0.296$ .

## 2. COLLISIONAL CROSS-SECTION ESTIMATES

The dark matter collisional cross-section,  $\sigma$ , can be constrained from the 1E 0657-56 data by at least four independent methods, using simple calculations described in the sections below. They are based on the observed gas–dark matter offset, the absence of an offset between the dark matter and the galaxies, the high subcluster velocity, and the subcluster survival. First, we list the main assumptions about 1E 0657-56 that go into these estimates.

There are two estimates of the total masses of the subcluster and the main cluster — from the galactic velocity dispersion (Barrena et al. 2002) and from weak lensing (C03). Given the disturbed state of this system, virial or hydrostatic mass estimates (either from galaxy velocities or the gas temperature) can be incorrect, and we chose to use the direct weak lensing measurements from C03 even though their formal statistical accuracy is poorer. The main cluster’s lensing signal can be fit by a King mass profile  $\rho = \rho_0(1 + r^2/r_c^2)^{-3/2}$  with best-fit pa-

<sup>1</sup> Harvard-Smithsonian Center for Astrophysics, 60 Garden St., Cambridge, MA 02138; maxim@head-cfa.harvard.edu

<sup>2</sup> Department of Astronomy, University of Florida

<sup>3</sup> Institut für Astrophysik und Extraterrestrische Forschung der Universität Bonn, Germany

<sup>4</sup> IKI, Moscow, Russia

<sup>5</sup> University of California at San Diego

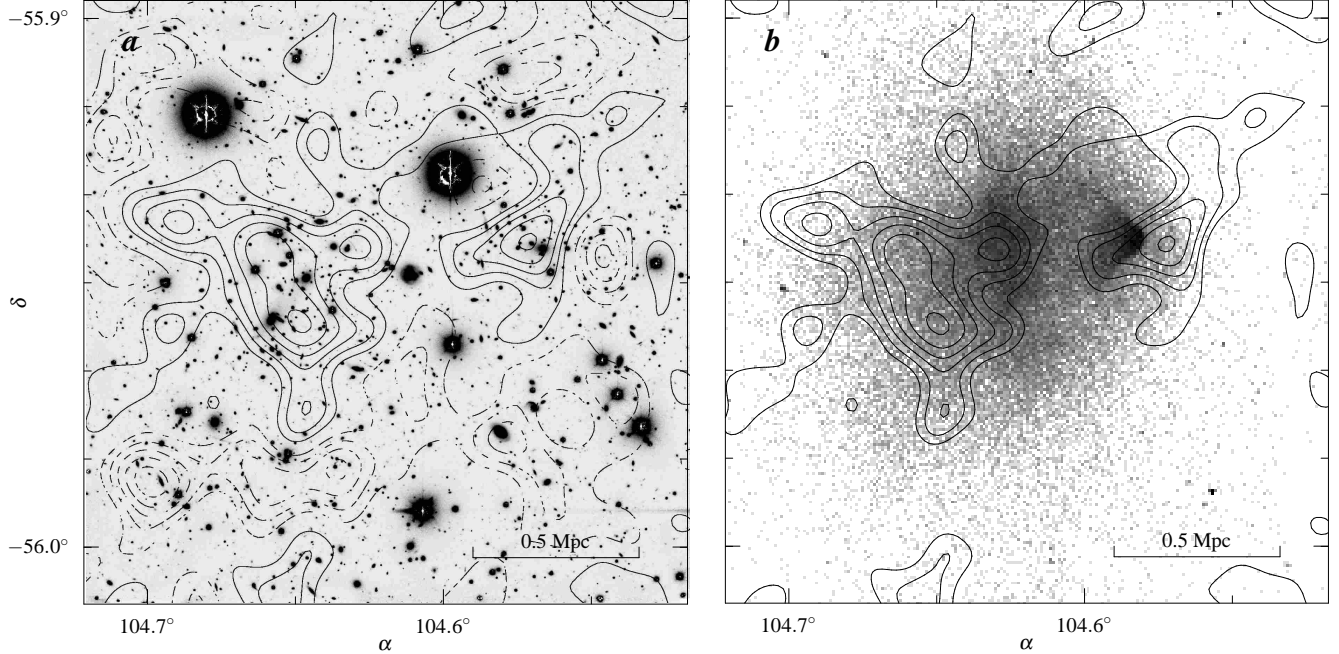


FIG. 1.— (a) Overlay of the weak lensing mass contours on the optical image of 1E 0657–56. Dashed contours are negative (relative to an arbitrary zero level). The subcluster's DM peak is coincident within uncertainties with the centroid of the galaxy concentration. (b) Overlay of the mass contours on the X-ray image (only the upper 5 of those in panel *a* are shown for clarity). The gas bullet lags behind the DM subcluster.

rameters  $\rho_0 = 2.6 \times 10^{-25} \text{ g cm}^{-3}$  and  $r_c = 210 \text{ kpc}$ . These two parameters are degenerate so their individual error bars are not meaningful; the quantity of interest to us is the central mass column density (approximately proportional to  $\rho_0 r_c$ ), which is measured with a  $6.5\sigma$  accuracy. This mass profile is very close to the Barrena et al. NFW profile at all radii outside the core. A King profile is marginally preferred over an NFW profile (also acceptable statistically). For our purposes, we can ignore marginally significant nonuniformities seen in the main cluster region of the lensing map (Fig. 1*a*).

The projected mass excess created by the subcluster is detected in the lensing data with a  $3.6\sigma$  significance. The lensing data accuracy is not sufficient to derive an exact mass distribution for the subcluster, but our estimates below are not very sensitive to it, being mostly determined by its overall projected mass. For the sake of modeling, we will use a best-fit King profile with  $\rho_0 = 2.0 \times 10^{-24} \text{ g cm}^{-3}$  and  $r_c = 54 \text{ kpc}$ . The subcluster mass signal extends to  $r_{\text{tr}} \approx 200 \text{ kpc}$ , which is likely the subcluster's tidal truncation radius after core passage (C03). The lensing-derived subcluster mass is significantly higher (by about a factor of 4) than the Barrena et al. estimate, but the latter result was based on only 7 galaxies and can easily be biased low because of the difficulty of identifying the subcluster members among all the cluster galaxies.

The subcluster is assumed to have passed (once) close to the center of the main cluster, as discussed above. The accuracy of our qualitative cross-section estimates will be determined by the validity of this and other assumptions (given below where relevant) to a greater degree than by the measurement uncertainties, so below we will omit the measurement error propagation for clarity.

### 2.1. The gas — dark matter offset

The most remarkable feature in Fig. 1*b* is a  $23^{+7}_{-11}$  arcsec offset between the subcluster's DM centroid and the gas bul-

let (C03). C03 use this fact as a direct proof of dark matter existence, as opposed to modified gravity hypotheses (Milgrom 1983 and later works). For our purposes, this offset means that the scattering depth of the dark matter subcluster w.r.t. collisions with the flow of dark matter particles cannot be much greater than 1. Otherwise the DM subcluster would behave as a clump of fluid, experiencing stripping and drag deceleration, similar to that of the gas bullet (assuming the same gas mass fraction in the main cluster and the subcluster), and there would be no offset between the gas and dark matter. The subcluster's scattering depth is

$$\tau_s = \frac{\sigma}{m} \Sigma_s, \quad (1)$$

where  $\sigma$  is the DM collision cross-section,  $m$  is its particle mass, and  $\Sigma_s$  is the DM mass surface density of the subcluster. For our adopted truncated King profile, the surface density averaged over the face of the subcluster within  $r < r_{\text{tr}}$  is  $\Sigma_s \simeq 0.1 \text{ g cm}^{-2}$ . Requiring  $\tau_s < 1$ , we obtain

$$\frac{\sigma}{m} < 10 \text{ cm}^2 \text{ g}^{-1}. \quad (2)$$

The surface density toward the subcluster center is several times higher, so by using an average we obtain a conservative upper limit.

From the gas–DM offset, one can devise another constraint based on the balance of forces on the gas bullet — the drag force due to the ambient gas ram pressure and the gravitational force from the offset subcluster mass, which can both be derived from the data. These forces are equal within the measurement errors, which places an upper limit on the DM clump deceleration and, therefore, drag from the DM particle collisions. However, for even a remotely interesting cross-section limit, we need a more accurate knowledge of the subcluster mass profile.

## 2.2. The high velocity of the subcluster

The observed velocity of the subcluster,  $v_s = 4500 \text{ km s}^{-1}$ , is in good agreement with the expected free-fall velocity onto the main cluster. For our main cluster's mass profile, a small subcluster falling from a large distance should acquire  $4400 \text{ km s}^{-1}$  at core passage, decelerating to  $3500 \text{ km s}^{-1}$  at the current  $0.66 \text{ Mpc}$  off-center distance of the subcluster. Since the cluster peculiar velocities are small, such an agreement strongly suggests that the subcluster could not have lost much of its momentum to drag forces. Drag is created by putative DM particle collisions, as well as the gravitational pull of the gas being stripped from the subcluster and of the tidally-stripped outer subcluster mass, and by dynamical friction as the moving subcluster disturbs the main cluster's matter distribution. We will conservatively disregard the latter three (which are not very strong effects) and assume, for a qualitative estimate, that the loss of velocity due to the DM collisions, compared to free fall, is less than  $1000 \text{ km s}^{-1}$ , accumulated along the way through the main cluster.

The subcluster will be decelerated by DM particle collisions when its DM particles acquire a momentum component opposite to the subcluster's velocity and then transfer all or part of it to the whole subcluster via gravitational interactions. To evaluate this effect, we assume for simplicity that (a) dark matter particles have no peculiar velocities, and (b) the subcluster's gravity is felt by the particles, and vice versa, as long as the particle is within a fiducial radius  $r' = 2r_{\text{tr}}$  of the subcluster (the result will not depend qualitatively on  $r'$  in the range  $r_{\text{tr}} - \infty$ ). We further assume that a particle transfers all of its momentum to the subcluster if its post-collision velocity is insufficient to escape beyond  $r'$  (in this Section, we are not interested whether it then falls back onto the subcluster or leaves for the main cluster). Faster-scattered particles retard the cluster only until they reach  $r'$ . We make another simplifying assumption that all collisions occur at the subcluster center, and use a mass-averaged *rms* value for the assumed subcluster mass profile,  $V \simeq 1800 \text{ km s}^{-1}$ , as the critical velocity that a particle needs to reach  $r'$  from there. We also conservatively disregard multiple scattering in the subcluster (the adequacy of this assumption is addressed below).

An elastic collision of two equal-mass particles proceeds as shown in Fig. 2. In the subcluster's reference frame, particle 2 is at rest and particle 1, in the incoming flow, collides with it with a velocity

$$v_0 = \sqrt{v_s^2 + V^2} \approx 4800 \text{ km s}^{-1}, \quad (3)$$

where  $v_s$  is the subcluster's velocity and the relatively small increase is because of the subcluster's gravitational pull within  $r = r'$ . Particle 1 scatters at an angle  $\alpha_1 > 0$  with

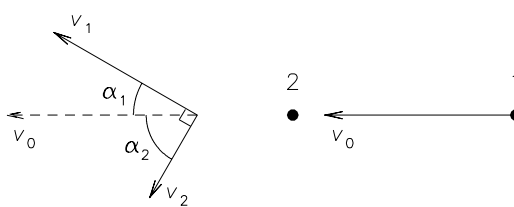


FIG. 2.— Collision of two equal-mass particles in the subcluster reference frame.

a velocity  $v_1$ , while particle 2 acquires a velocity  $v_2$  at an angle  $\alpha_2 > 0$ . From energy and momentum conservation,  $\alpha_1 + \alpha_2 = \pi/2$  and the velocities are

$$v_1 = v_0 \cos \alpha_1, \quad v_2 = v_0 \sin \alpha_1. \quad (4)$$

As a result of each collision, the subcluster acquires a net momentum along the  $v_0$  direction,  $p = p_0 + p_1 + p_2$ , where

$$p_0 = m(v_s - v_0) \quad (5)$$

comes from the infalling particle (which carries back exactly  $-p_0$  if it passes through the subcluster without scattering), and  $p_i$  ( $i = 1, 2$ ) comes from the respective outbound particle. If  $v_i < V$  then

$$p_i = m v_i \cos \alpha_i \quad (6)$$

(the particle transfers all its momentum to the subcluster), while for  $v_i > V$ ,

$$p_i = m \left[ v_i - (v_i^2 - V^2)^{1/2} \right] \cos \alpha_i. \quad (7)$$

For our particular mass and velocity, at least one particle always escapes beyond  $r'$ . If both escape, which occurs in collisions with  $\alpha_e < \alpha_1 < \frac{\pi}{2} - \alpha_e$  ( $\alpha_e \simeq 22^\circ$  for our parameters), the momentum loss by the subcluster as a function of the scattering angle  $\alpha_1$  is (combining eqs. 5, 7, 3, and 4):

$$p_{\text{both}} = m v_s \left[ 1 - \cos \alpha_1 \left( \cos^2 \alpha_1 - \frac{V^2}{v_s^2} \sin^2 \alpha_1 \right)^{1/2} - \sin \alpha_1 \left( \sin^2 \alpha_1 - \frac{V^2}{v_s^2} \cos^2 \alpha_1 \right)^{1/2} \right]. \quad (8)$$

If only one particle escapes, which occurs in two symmetric cases,  $0 < \alpha_1 < \alpha_e$  or  $\frac{\pi}{2} - \alpha_e < \alpha_1 < \frac{\pi}{2}$ , the net momentum loss is (combining eqs. 5, 6, 7, 3, and 4):

$$p_{\text{one}} = m v_s \left[ 1 - \cos \alpha_1 \left( \cos^2 \alpha_1 - \frac{V^2}{v_s^2} \sin^2 \alpha_1 \right)^{1/2} \right]. \quad (9)$$

We would like to average the above momentum loss over all scattering angles. For this, it is convenient to use the reference frame of the center of mass of the colliding particles. In this frame, the scattering is isotropic, as long as the particles are “slow” in the sense that  $mvr/\hbar \ll 1$ , where  $r$  is the linear scale of the interaction and  $v$  is the collision velocity (Landau & Lifshitz 1958, §132). For example, for rigid spheres with radius  $r$  (for which the scattering cross-section is  $\sigma = 4\pi r^2$ , Landau & Lifshitz 1958), the scattering is isotropic if

$$\left( \frac{mc^2}{1 \text{ GeV}} \right)^{3/2} \left( \frac{v}{2200 \text{ km s}^{-1}} \right) \left( \frac{\sigma/m}{50 \text{ cm}^2 \text{ g}^{-1}} \right)^{1/2} \ll 1 \quad (10)$$

(the collision velocity in this reference frame is  $v = v_0/2$ ). Note that if the DM particles are WIMPs with the currently favored mass ( $mc^2 > 40 \text{ GeV}$ , Hagiwara et al. 2002), this condition is not satisfied for the values of  $\sigma/m \sim (1 - 10) \text{ cm}^2 \text{ g}^{-1}$  that we are able to constrain. Scattering with such combination of  $\sigma$  and  $m$  would be strongly beamed, reducing all the observable effects for a given  $\sigma$ . However, there is still ample parameter space for isotropic scattering (e.g., if particles are not WIMPs), and we will confine our estimates to this simple case.<sup>6</sup>

<sup>6</sup> Note that our conclusions will be directly comparable to other astrophysical cross-section measurements which also implicitly assume isotropic scattering.

In the center-of-mass reference frame, particle 1 scatters by an angle  $\theta = 2\alpha_1$  ( $0 < \theta < \pi$ ) and particle 2 scatters by  $\pi - \theta$ . Combining eqs. (8, 9), weighting with solid angle and taking into account the symmetries, the average momentum lost by the subcluster in each particle collision is (for our values of  $V$  and  $v_s$ ):

$$\bar{p} = mv_s \left[ 1 - 4 \int_{\sin \alpha_e}^1 x^2 \left\{ x^2 - \frac{V^2}{v_s^2} (1 - x^2) \right\}^{1/2} dx \right] \approx 0.1 mv_s. \quad (11)$$

When the subcluster with mass  $M_s$  (all in the form of dark matter for clarity) travels with a velocity  $v$  through the main cluster with density  $\rho_m$ , it experiences

$$n = \frac{M_s}{m} \frac{\sigma}{m} \rho_m v \quad (12)$$

collisions per second. As a result, it loses velocity (relative to the free-fall velocity  $v_{ff}$ ):

$$\frac{d(v - v_{ff})}{dt} = \frac{\bar{p}n}{M_s} = \frac{\bar{p}}{m} \frac{\sigma}{m} \rho_m v, \quad (13)$$

where  $\bar{p}$  is from eq. (11). We assume that the loss of mass and velocity is relatively small, so  $\bar{p}$  is roughly constant (which also conservatively disregards the higher subcluster velocity during core passage), and integrate eq. (13) along the trajectory to calculate the total velocity loss. Noting that  $\int \rho_m v dt = \int \rho_m dl = \Sigma_m$ , the mass column density of the main cluster along the subcluster's trajectory, we obtain, for the present subcluster location,

$$v - v_{ff} = \frac{\bar{p}}{m} \frac{\sigma}{m} \Sigma_m. \quad (14)$$

Almost all of  $\Sigma_m$  accumulates within the main cluster's core, at distances smaller than the current subcluster position. If, as we assume, the subcluster passed through the main cluster center,  $\Sigma_m \simeq 0.3 \text{ g cm}^{-2}$ ; if it missed the center by 200–300 kpc,  $\Sigma_m$  is lower by about a factor of 2. On the other hand, we observe the main cluster after the collision; if it used to have an NFW-type peak disrupted by a direct hit of the subcluster, then  $\Sigma_m$  that we should use would be higher than the observed one.

Requiring that  $v - v_{ff} < 1000 \text{ km s}^{-1}$ , from eq. (14) we get

$$\frac{\sigma}{m} < 7 \text{ cm}^2 \text{ g}^{-1}. \quad (15)$$

### 2.3. No offset between the dark matter and the galaxies

Another remarkable feature in Fig. 1a is the coincidence of the subcluster dark matter centroid with that of the galaxy distribution, to within their uncertainties. Suppose the DM particles are experiencing frequent collisions and a resulting displacement. The galaxies, which are sparse and effectively collisionless, need time to redistribute over the subcluster and come into equilibrium with a DM gravitational potential that is lagging behind. This timescale is at least  $r_{tr}/v_r \approx 3 \times 10^8 \text{ yr}$ , where  $v_r \simeq 700 \text{ km s}^{-1}$  is the radial velocity dispersion for the observed subcluster mass. If, on this timescale, *most* of the subcluster's DM particles experience another collision, there would be a persistent offset between the galaxy and DM peaks, just like that observed between the DM and the X-ray gas. During the past  $3 \times 10^8 \text{ yr}$ , the subcluster has traveled  $\sim 1.3 \text{ Mpc}$ , passing through most of the main cluster's observed mass column  $\Sigma_m$ . For each DM particle presently in the subcluster, the collision probability has been

$$\tau_m = \frac{\sigma}{m} \Sigma_m. \quad (16)$$

Simply requiring that this probability is less than 1, we obtain

$$\frac{\sigma}{m} < 3 \text{ cm}^2 \text{ g}^{-1}. \quad (17)$$

We should emphasize here that the subcluster galaxies, although effectively collisionless, do not give us the position at which the subcluster would be found in the absence of DM collisions, because the galaxies are gravitationally bound to the DM clump. Indeed, e.g., for  $\sigma/m = 3 \text{ cm}^2 \text{ g}^{-1}$ , from eq. (14) integrated over the trajectory, this “free-fall” position would be  $\sim 60 \text{ kpc}$  ahead of the current DM and galaxy centroids, comparable to the distance between the gas bullet and the DM clump.

### 2.4. The survival of the dark matter subcluster

For the observed subcluster mass and velocity, the most likely result of a particle collision is the loss of a particle by the subcluster. The velocity that the subcluster particles need to escape beyond  $r = r_{tr}$  is  $v_{esc} \simeq 1300 \text{ km s}^{-1}$  (averaged over the subcluster). From eq. (4),  $v_2$  becomes greater than  $v_{esc}$  starting from small scattering angles for the infalling particle 1,  $\alpha_1 \gtrsim 15^\circ$ . The opposite effect, i.e., accretion of the main cluster's particles, is negligible because of the low mass and high velocity of the subcluster.

We can put an upper limit on the accumulated mass loss and thereby on the collision cross-section. C03 have derived a *B*-band mass-to-light ratio for the subcluster within its truncation radius,  $M/L \simeq 260 \pm 90$ , which is in good agreement with the universal cluster value from the lensing analyses (e.g., Mellier 1999), and a factor of  $1.1 \pm 0.3$  from the main cluster value derived from the same data (where the error is from the mass measurements). If the subcluster had been continuously losing DM particles, and given the long timescale on which its galaxies would evaporate from the slowly diminishing gravitational well (§2.3), we would expect an anomalously low  $M/L$  value for the subcluster — and in particular, a value lower than the main cluster  $M/L$  ratio. Note that although the main cluster's particles are similarly affected by the subcluster impact, the effect on the main cluster  $M/L$  value is smaller by at least their mass ratio (about a factor of 6). From this agreement we can infer that the subcluster could not have lost more than  $\mu \approx 0.2–0.3$  of its initial mass within  $r_{tr}$ .

The subcluster loses a particle in a collision if both  $v_1 > v_{esc}$  and  $v_2 > v_{esc}$ , which occurs at scattering angles  $\theta$  given by (from eqs. 4):

$$\frac{v_{esc}}{v_0} < \sin \frac{\theta}{2} < \left( 1 - \frac{v_{esc}^2}{v_0^2} \right)^{1/2}. \quad (18)$$

The probability of this happening, per collision, is

$$\chi = \frac{\int_{(18)} 2\pi \sin \theta d\theta}{\int_0^\pi 2\pi \sin \theta d\theta} = 1 - 2 \frac{v_{esc}^2}{v_0^2}, \quad (19)$$

where the upper integral is calculated over the interval of  $\theta$  given by eq. (18). During the subcluster's transit through the main cluster, each of its original particles has a probability to collide  $\tau_m$  given by eq. (16). Combining (19) and (16), the fraction of particles lost is

$$\chi \tau_m = \frac{\sigma}{m} \Sigma_m \left[ 1 - 2 \left( \frac{v_{esc}'}{v_0} \right)^2 \right]. \quad (20)$$

Here we allow for the subcluster's mass to decline by up to a factor of  $1 + \mu$  along the way; its escape velocity would also

decline, so we must (conservatively) use a slightly higher average  $v'_{\text{esc}} \approx v_{\text{esc}}(1 + \sqrt{1 + \mu})/2$ . At the same time, we conservatively ignore the subcluster's higher velocity at core passage, assuming the constant present velocity. (Both effects are small.) Requiring that  $\chi\tau_m < \mu = 0.3$ , from eq. (20) we obtain

$$\frac{\sigma}{m} < 1 \text{ cm}^2 \text{ g}^{-1}. \quad (21)$$

A more conservative limit, independent of the  $M/L$  measurements, can be placed simply from the requirement (which follows from the X-ray and optical data) that the two subclusters have had different pre-merger masses. At present, the mass of the main cluster within a radius of 0.5 Mpc (the distance toward the subcluster where the lensing map starts showing the presence of the subcluster) is about 6 times the mass of the subcluster within its  $r_{\text{tr}}$ . If we assume that the initial subcluster mass ratio was at least 2:1, then the subcluster could not have lost more than  $\mu = 2/3$  of its initial mass, which gives a limit of  $\sigma/m < 3 \text{ cm}^2 \text{ g}^{-1}$ .

For cross-sections such as (17) and (21) and the subcluster's observed mass and radius, the mean scattering depth of the subcluster is  $\tau_s \lesssim 0.3$ . Thus our single-scattering assumption is reasonable as a first approximation. If one considers a possibility that the escaping particle may expel another subcluster particle, the probability (20) is a conservative underestimate. In §2.2, even higher  $\tau_s$  are allowed by our resulting limit (15); for that method, single scattering is also a conservative assumption. Inclusion of multiple scattering would lead to tighter limits, but requires detailed knowledge of the matter distribution inside the subcluster and is not warranted by the present data.

### 3. DISCUSSION

From our order-of-magnitude estimates, the most promising way of improving the limit on (or measuring) the DM collision cross-section using 1E 0657–56 would be to refine the weak lensing mass map and limit (or detect) the mass loss from the subcluster core. Indeed, if it had lost a significant fraction of its DM particles, they should form a tail detectable in the dark matter map, not unlike the X-ray gas tail. This would of course overlay on the tidally stripped matter and a gravitational wake discussed by Furlanetto & Loeb (2002). The main cluster's DM particles also would be scattered, probably resulting in additional detectable effects in the mass map. These considerations, along with the conservative assumptions that we made to simplify calculations (esp. in §2.2), suggest that the best way to proceed with the data interpretation is a detailed hydrodynamic simulation of this merger (whose masses, geometry and velocity are quite clear), such as that performed by Tormen, Moscardini, & Yoshida (2003) but with the inclusion of collisionless galaxies and collisional DM with various cross-sections, followed by comparison of the results with the X-ray, optical and lensing data.

#### 3.1. Astrophysical context

Laboratory experiments showed that interaction between the dark and baryon matter is vanishingly small, with cross-sections many orders of magnitude lower than the values we consider in this work (e.g., Bernabei et al. 2003 and references therein). Despite their size, galaxy clusters, including 1E 0657–56, have an average projected mass density of at most  $0.1 - 1 \text{ g cm}^{-2}$ , so they are no match to the laboratory experiments for constraining the DM-baryon interactions. How-

ever, they may provide the best available setup for studying the DM self-interaction.

While the common wisdom is that DM is collisionless, a hypothesis of self-interacting dark matter (SIDM) with cross-sections of order  $1 - 100 \text{ cm}^2 \text{ g}^{-1}$  was most recently proposed by Spergel & Steinhardt (2000) to alleviate several apparent problems of the collisionless CDM model, such as non-observation of the predicted cuspy mass profiles in galaxies (e.g., Moore 1994; Flores & Primack 1994; cf. Navarro, Frenk, & White 1997; Moore et al. 1999b) and over-prediction of small sub-halos within the larger systems (e.g., Klypin et al. 1999; Moore et al. 1999a). Simulations and theoretical studies (e.g., Davé et al. 2001; Ahn & Shapiro 2002) narrowed the range required to explain the galaxy profiles to  $\sigma/m \sim 0.5 - 5 \text{ cm}^2 \text{ g}^{-1}$  and pointed out that fluid-like DM with  $\sigma/m \sim 10^4 \text{ cm}^2 \text{ g}^{-1}$  is another possibility.

Several observational constraints have been reported. Gnedin & Ostriker (2001; see also Hennawi & Ostriker 2002) pointed out that unless  $\sigma/m < 0.3 - 1 \text{ cm}^2 \text{ g}^{-1}$ , galactic halos inside clusters should evaporate on the Hubble timescale, because of collisional heat conduction from the hot cluster DM particles into the cool halos. We note that our constraint in §2.4 uses essentially the same idea, except that we consider a cluster-sized halo subjected to a flow of particles from one direction instead of isotropic bombardment. (The latter difference offers a potential advantage — as mentioned above, one will know where to look for the expelled particles to obtain a tighter constraint.)

Furlanetto & Loeb (2002) proposed to use the different shapes of a gravitational wake that a moving halo would create in the collisionless and fluid-like DM models. They argue that the X-ray image of the bright galaxy in the Fornax cluster already disfavors fluid-like DM. Their method is somewhat similar to our 1E 0657–56 estimates in that it also uses the motion of a halo within a bigger halo, but appears more observationally challenging. Following another suggestion of Furlanetto & Loeb (2002), Natarajan et al. (2002) used observed sizes of the galactic halos in the A2218 cluster (which should be truncated at different radii for different DM cross-sections) to obtain  $\sigma/m < 40 \text{ cm}^2 \text{ g}^{-1}$ . Upper limits in the  $0.02 - 10 \text{ cm}^2 \text{ g}^{-1}$  range were derived by Hennawi & Ostriker (2002) from the absence of supermassive black holes in the centers of galaxies.

Strong constraints are reported from the galaxy cluster cores. Yoshida et al. (2000) simulated a cluster mass profile for  $\sigma/m = 10, 1, \text{ and } 0.1 \text{ cm}^2 \text{ g}^{-1}$  and obtained systematically flatter profiles for higher  $\sigma/m$ . Using *Chandra* X-ray data and the assumption of hydrostatic equilibrium, Arabadjis et al. (2002) derived a mass profile for the cluster MS 1358+62 that is strongly centrally peaked (in fact, more peaked than even the collisionless simulations predict). From the comparison with Yoshida et al. (2000), they conclude that  $\sigma/m < 0.1 \text{ cm}^2 \text{ g}^{-1}$ . There are two potential difficulties with this stringent limit, however. *Chandra* revealed widespread gas sloshing in the cores of “relaxed” clusters (Markevitch, Vikhlinin, & Forman 2002), including in MS 1358+62, which does not lend support to the hydrostatic equilibrium assumption and the resulting X-ray mass estimates at relevant radii. More importantly, Yoshida et al. present time evolution of their simulated cluster profile for  $\sigma/m = 10 \text{ cm}^2 \text{ g}^{-1}$ , which at different epochs covers a range of shapes comparable to the whole difference between their 0.1 and  $10 \text{ cm}^2 \text{ g}^{-1}$  simulations (see also Hennawi & Ostriker 2002). This suggests that for a high  $\sigma/m$ ,

one expects a variety of cluster mass profiles — and indeed, a large fraction of the real clusters have flat cores (e.g., Coma), while many others exhibit peaked profiles. Obviously, a sample of cluster profiles is required for such studies. Miralda-Escudé (2002) used lensing data for the cluster MS 2137–23 to show that its central mass distribution is elliptical, and concluded that  $\sigma/m < 0.02 \text{ cm}^2 \text{ g}^{-1}$ , since otherwise DM collisions would erase ellipticity. Again, this interpretation may not be unique, because ellipticity may be affected by line-of-sight projections. This ambiguity is illustrated by the fact that Sand et al. (2002), using lensing data for the same cluster but considering the flatness of the central mass distribution instead of its ellipticity, arrived at the opposite conclusion.

While the above methods may eventually provide more sensitive constraints on  $\sigma/m$  than we have obtained, they require a statistical sample of clusters and cosmological simulations to reach solid conclusions. In comparison, the unique setup of the 1E 0657–56 cluster merger allows us to see directly the (cumulative) results of single DM particle collisions, which

makes the resulting limits quite robust.

#### 4. SUMMARY

We have combined new X-ray, optical and weak lensing observations of the unique merging cluster 1E 0657–56 to derive a simple, direct upper limit on the dark matter collisional cross-section,  $\sigma/m < 1 \text{ cm}^2 \text{ g}^{-1}$ . This is only an order-of-magnitude estimate; a more accurate, and quite possibly stronger, limit may be derived through hydrodynamic simulations of this merger.

Support for this work was provided by NASA contract NAS8-39073, *Chandra* grant GO2-3165X, and the Smithsonian Institution. AHG was supported under award AST-0201355 by an NSF AAPF; DC received support from Deutsche Forschungsgemeinschaft under the project SCHN 342/3-1.

#### REFERENCES

Ahn, K., & Shapiro, P. R. 2002, J. Korean Astronomical Soc., 35, 1  
 Arabadjis, J. S., Bautz, M. W., & Garmire, G. P. 2002, ApJ, 572, 66  
 Barrena, R., Biviano, A., Ramella, M., Falco, E. E., & Seitz, S. 2002, A&A, 386, 816  
 Bernabei, R., et al. 2003, preprint astro/ph-0307403  
 Clowe, D., et al. 2003, in preparation (C03)  
 Davé, R., Spergel, D. N., Steinhardt, P. J., & Wandelt, B. D. 2001, ApJ, 547, 574  
 Flores, R. A., & Primack, J. R. 1994, ApJ, 427, L1  
 Furlanetto, S. R., & Loeb, A. 2002, ApJ, 565, 854  
 Gnedin, O. Y., & Ostriker, J. P. 2001, ApJ, 561, 61  
 Hagiwara, K., et al. 2002, Phys. Rev. D, 66, 10001  
 Hennawi, J. F., & Ostriker, J. P. 2002, ApJ, 572, 41  
 Klypin, A., Kravtsov, A. V., Valenzuela, O., & Prada, F. 1999, ApJ, 522, 82  
 Landau, L. D., & Lifshitz, E. M. 1958, Quantum mechanics: non-relativistic theory (London: Pergamon)  
 Liang, H., Hunstead, R. W., Birkshaw, M., & Andreani, P. 2000, ApJ, 544, 686  
 Markevitch, M., Gonzalez, A. H., David, L., Vikhlinin, A., Murray, S., Forman, W., Jones, C., & Tucker, W. 2002, ApJ, 567, L27 (M02)  
 Markevitch, M., Vikhlinin, A., & Forman, W. 2002, astro-ph/0208208  
 Markevitch, M., et al. 2003, in preparation (M03)  
 Mellier, Y. 1999, ARA&A, 37, 127  
 Milgrom, M. 1983, ApJ, 270, 365  
 Miralda-Escudé, J. 2002, ApJ, 564, 60  
 Moore, B. 1994, Nature, 370, 629  
 Moore, B., Ghigna, S., Governato, F., Lake, G., Quinn, T., Stadel, J., & Tozzi, P. 1999a, ApJ, 524, L19  
 Moore, B., Quinn, T., Governato, F., Stadel, J., & Lake, G. 1999b, MNRAS, 310, 1147  
 Natarajan, P., Loeb, A., Kneib, J., & Smail, I. 2002, ApJ, 580, L17  
 Navarro, J. F., Frenk, C. S., & White, S. D. M. 1997, ApJ, 490, 493  
 Sand, D. J., Treu, T., & Ellis, R. S. 2002, ApJ, 574, L129  
 Spergel, D. N., & Steinhardt, P. J. 2000, Phys. Rev. Lett., 84, 3760  
 Tormen, G., Moscardini, L., & Yoshida, N. 2003, MNRAS, submitted (astro-ph/0304375)  
 Tucker, W. H., Tananbaum, H., & Remillard, R. A. 1995, ApJ, 444, 532  
 Yoshida, N., Springel, V., White, S. D. M., & Tormen, G. 2000, ApJ, 544, L87